

Effect of Frost Growth on Performance of Cooled Flat Surface

تأثير نمو طبقة الجليد على أداء سطح أفقى بارد

Mohammed J. H. Alkandari

Alkwait

فى هذه الدراسة تم عمل نموذج معملى لانتقال الحرارة والكتلة لهواء رطب يمر على سطح بارد مع تكون صقيع. وتم تصميم وتنفيذ دائرة تبريد وتزويدها بأجهزة قياس لدرجة حرارة السطح البارد وكذلك قياس وكتلة الماء ودرجة حرارة الهواء الداخلى والخارج من مقطع الاختبار. وتم عمل التجارب كلها فى ظروف ثابتة لدرجة حرارة الهواء الداخلى الى مقطع الاختبار. وقد بينت هذه الدراسة مع تكون طبقة الجليد على سطح المبخر يقل معامل انتقال الحرارة والكتلة وكذلك رقمى نسلت وشيروود

Abstract

The present work is an experimental investigation of heat and mass transfer with frost growth over flat plate surface. This study focuses on the most important factors affecting the frost formation process, i.e. the surrounding air temperature, air humidity and air velocity, and the plate surface temperature. Experiments were carried out using a purpose-built apparatus to acquire data to measure the thickness of frost layer, and surface temperature of frost layer. Results showed that the plate surface temperature and air velocity have the greatest effect on frost layer thickness and heat and mass transfer coefficients, relative to the air humidity and air temperature. Comparisons between present exponential results and previous work relevant to this study show a fairly good agreement.

KEY WORDS: heat and mass transfer, frost layer thickness, cold flat surface

Nomenclature

A	Duct area, m ²
A _s	Cooled plat surface area, m ²
D	Diffusivity of water vapor in air, m ² s ⁻¹
h _m	Mass transfer coefficient, m s ⁻¹
h _h	Heat transfer coefficient, W m ⁻² K ⁻¹
i	Moist air enthalpy, J kg ⁻¹
K	Thermal conductivity, W m ⁻¹ K ⁻¹
L	Length of cooled plate, m
\dot{m}	Mass flow rate, kg s ⁻¹
\dot{m}''	Mass flux, kg m ⁻² s ⁻¹
q''	Heat flux (W m ⁻²)
T	Temperature (K)
t	Time (min)
u	Air velocity (m s ⁻¹)

Greek symbols

ν	Kinematic viscosity, m ² s ⁻¹
ω	Absolute humidity, kg kg _a ⁻¹
ρ	Density, kg m ⁻³
Δ	Quantity difference between inlet and outlet

Subscripts

a	Air
av	Average
fs	Frost surface
s	Surface

Dimensionless number

Nu	Local Nusselt number
\overline{Nu}	Average Nusselt number
Sh	Local Sherwood number
\overline{Sh}	Average Sherwood number
Re	Reynolds number

1. Introduction

The frost formation and growth on cold surface influences the performance of heat exchanger, and then exerts a negative effect on the performance of the air source heat pump or refrigeration unit. It is important to understand the frost characteristics, such as the frost thickness, density, frost growth rate, frost surface temperature and heat flux. However, these frost characteristics are various under different frosting conditions, like different air temperature, relative air humidity, air velocity, temperature of the cold surface. Though a lot of literatures have been published to investigate the frosting characteristics by conducting experiments, it is still difficult to comprehensively understand the frosting mechanism only by experimental data. A simple model is required to predict the characteristics of frost growth under different conditions. Quite a few scholars have put forward some models to investigate the heat and mass transfer between moist air and frost surface. Kennedy and Goodman [1] Studied frost formation on a vertical surface under natural convection conditions. Hayashi et al. [2] divided the frost formation into three steps and proposed an empirical correlation to calculate the frost density. Schneider [3] Based on accurate measurements of a cooled tube found that the frost thickness turns out to be independent of the variables commonly significant on mass transfer, such

as Reynolds number and vapor pressure difference. Marinyuk [4] Studied the effect of frost formation on heat transfer between a test cylinder and its gaseous environment. Dietenberger [5] found that the thermal conductivity of the frost layer plays an important part in its structure and rate of formation. Sami and Duong [6] Developed an improved model to predict frost formation growth. Östin and Andersson [7] studied the formation of frost on parallel horizontal plates facing a forced air stream at varying temperatures, relative humidities and air velocities. Östin [8] Studied experimentally the influence of frost formation on the heat exchange surfaces. Tao et al [9] Simulated frost deposition on a cold surface exposed to a warm moist air flow using a one-dimensional, transient formulation based on the local volume averaging technique. Sherif et al [10] studied theoretically the frost formation process employing a semi-empirical transient model for a flat plate under forced convection conditions. Le Gall et al [11] Derived a one-dimensional transient formulation to predict frost growth and densification on a cold wall submitted to a moist air flow. Lee et al [12] Developed an analytical model for the formulation of a frost layer on a cold flat surface by considering the molecular diffusion of water, and heat generation due to the

sublimation of water-vapor in the frost layer. Ismail and Salinas [13] Studied numerically some of the parameters involved in modeling the process of frost formation on flat cold surfaces subject to the flow of humid air. Wu and Webb [14] studied experimentally the possibility of causing frost to release from a cold surface. Both hydrophilic and hydrophobic surfaces were examined. Cheng and Cheng [15] Developed a theoretical model for frost formation on a cold plate placed in atmospheric air. Fossa and Tanda [16] Studied experimentally frost growth on a vertical plate in free convection. Wang et al [17] develop a generalized model for predicting the frost growth on cold flat plate. Hermes et al [19] studied theoretically and experimentally frost growth and densification on the flat surface with tested plate dimensions (10 x 10 cm²).

In this paper, an experimental investigation was undertaken to characterize the effects of operating parameters on the frost layer thickness and heat and mass transfer coefficients in the frost layer over cooled flat surface. The operating parameters are air velocity, air humidity, air temperature and cooled plate surface temperature.

2. Experimental Test Rig

The experimental test rig is designed and constructed to study the effect of operating parameters on the frost formation process, i.e. the surrounding air temperature, air humidity, air velocity and the cold plate surface temperature. Figure (1) shows the cooled flat plat inside a rectangular duct.

The test rig consists of :

- i) Test section,
- ii) Coolant system,
- iii) Air system

2.1 Test section unit

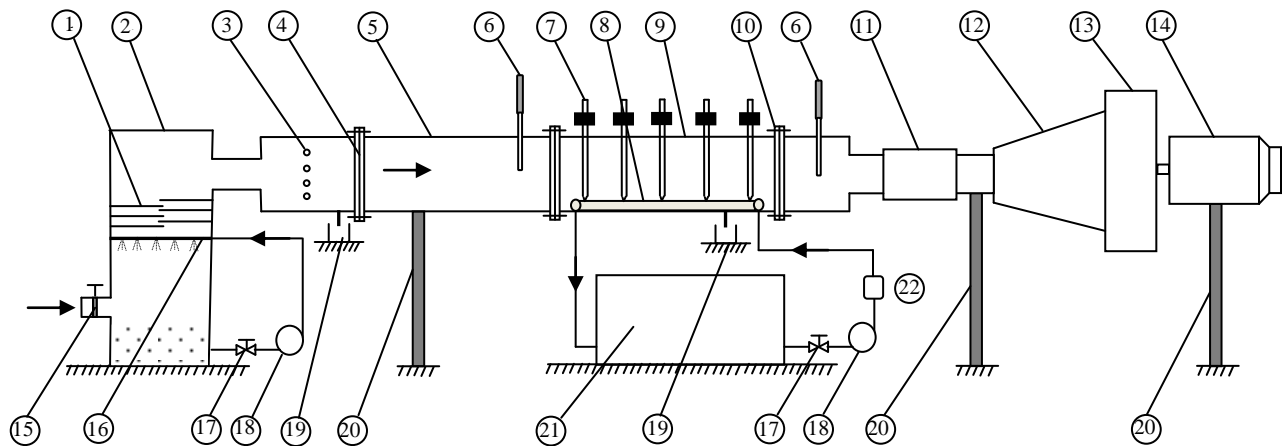
The test section unit shown in Fig (2) is considered the main item of the test rig. It contains a cooled flat plate made of aluminum. With a dimensions of (700 mm length x 200 mm width x 6mm thickness). The cooled Plat is mounted on the bottom wall of a rectangular duct which has dimensions of (1000 mm length x 300 mm width x 150 mm height).

2.2 coolant system

The coolant system is shown in Fig (3), and consists of the following matched systems:

2.2-a) Refrigeration system

Components of the refrigeration system were assembled together for decreasing Ethylene glycol solution temperature and consequently plat surface temperature to a sub zero degrees .The refrigeration system consists of a condensing unit contains a hermetic (R134a) compressor of an approximate power of (566 W) which is connected to an air cooled condenser of (9.5 mm) tube diameter and approximate pipe length of 7.0m, arranged in to six rows and two columns with a fin spacing of 3.0 mm .The approximate overall dimensions of the condenser are (300mm x 200mm x50mm).A fan motor of 25.0W was attached to the condenser with four blades made of aluminum. The system is equipped by a thermostatic expansion valve with external equalizer (Type: Danfoss brand-orifice 1).Smooth Copper tube evaporator coil of 15.87mm diameter and 5.0m length placed at the bottom of the insulated ethylene glycol solution tank.



- | | | |
|----------------------|--------------------------|-------------------------|
| 1 - Eliminator | 9 - Test section | 17 - Hand valve |
| 2 - Humidifier | 10 - Flange | 18 - Water pump |
| 3 - Electric heater | 11 - Flexible connection | 19 - Water pan |
| 4 - Screener | 12 - Expansion section | 20 - Stand bar |
| 5 - Entrance section | 13 - Centrifugal fan | 21 - Refrigeration unit |
| 6 - Hygrometer | 14 - Electric motor | 22 - Flow meter |
| 7 - Micrometer gage | 15 - Gate valve | |
| 8 - Cooled plate | 16 - Water spray | |

Fig.(1) Layout and components of the experimental test rig.

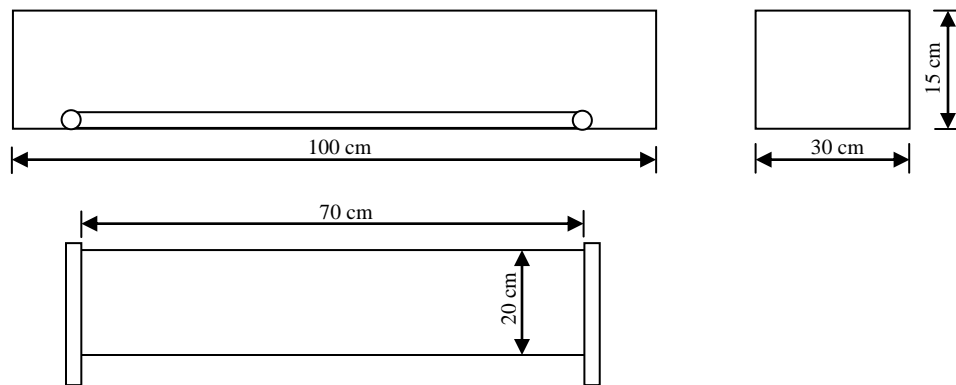


Fig. (2) Schematic diagram of test section and cooled flat plate.

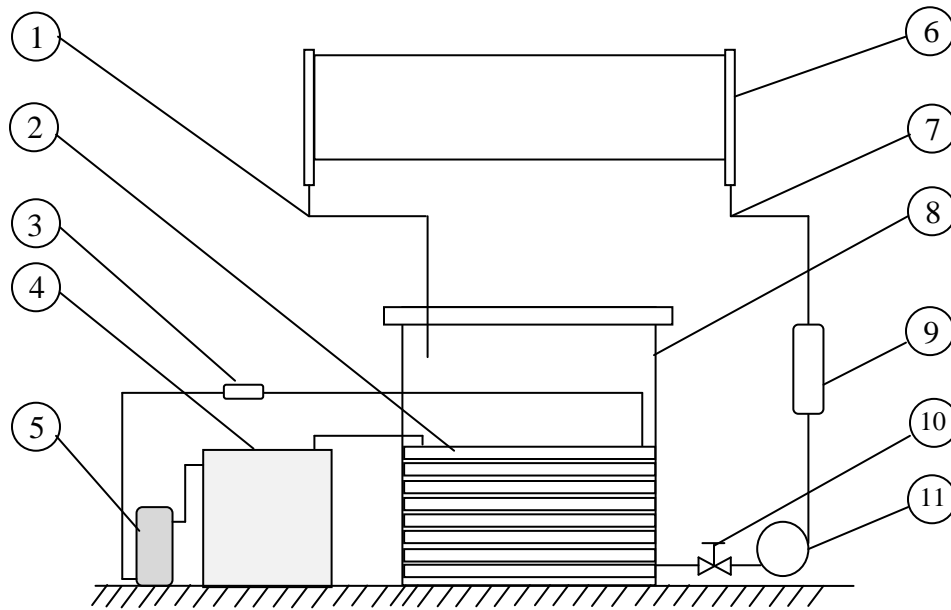
2.2-b) Ethylene-Glycol solution circulating system

The cooled Ethylene Glycol solution with 50% concentration is circulated by a small centrifugal pump of (335.6W). Inlet and outlet of the pump are both connected to an insulated (P.V.C.) pipes of (19.05 mm diameter) with suitable connectors. The

pump outlet is connected to a flow meter in order to measure ethylene glycol solution flow rate. The solution then is directed towards the cooled plate by passing through the inlet common header which is ended with a three (P.V.C) hand valves are mounted to deliver and control the solution flow to cooled plate with the aid of flexible

(9.5 mm) inner diameter pipes. An outlet common header is mounted to collect solution streams back to an insulated 150

liter source tank which feeds the pump again in a closed loop.



- | | | |
|-----------------------------------|----------------------------------|---------------------------|
| 1 - Glycol solution outlet header | 5 - Refrigerant liquid tank | 9 - Flow meter |
| 2 - Evaporator | 6 - Cooled plate | 10 - Hand valve |
| 3 - Expansion valve | 7 - Glycol solution inlet header | 11 - Glycol solution pump |
| 4 - Condensing unit | 8 - Glycol solution tank | |

Fig. (3) Cooling system arrangements

2.3 Air Flow System

The atmospheric air is sucked through a rectangular duct with a cross section area of (300mm x150mm) by the act of centrifugal fan (Fig .(1)). The duct is divided into three stages, the first is called the climitization section at which air is heated and humidified using a bank of electric heaters and humidifier in order to get a wider range of inlet air properties (temperature and moisture contents). While, the second is the test section of 1.0 m length (see Fig. 2).The third stage which extends to 1.0 m length is the stabilization section, Its function is to avoid the back pressure from the fan which is mounted at the end of the stage.

2.4 Experimental Procedures

The following procedures were held up to reach the required steady state condition just for the start of experiment as follows:

- 1- The Ethylene-glycol solution circulating system is turned "on", the solution flows from the insulated tank to the pump and back to the tank again with the aid of by-pass valves to get a good mixture of the solvent in water.
- 2- Turn the solution refrigerating system ON.
- 3- Switch ON the centrifugal fan with adjusting the regulator to the required velocity.
- 4- Switch on the electric pre-heaters and adjust its regulator.
- 5-Turning the humidification system – humidifier- "ON" and adjusting the water flow rate for the required relative humidity.
- 6-After the refrigeration unit reached the required Ethylene-glycol solution temperature (controlled by a digital

thermostat), the by-pass system changed the flow of solution towards the plat.

- 7- Measure Ethylene-glycol solution flow rate by the flow meter.
- 8- Start the digital stop watch as the experiment is started and the following thermocouples' temperatures are recorded as follows:
 - a- Inlet and outlet solution temperatures from and to plat.
 - b- flat plate surface temperature is recorded by using the temperature recorder.
- 9- Inlet and outlet dry bulb and dew point temperatures of moist air are measured by a digital thermo-hygrometer (testo 605-H1) with a resolution of 0.1 °C and accuracy of ±0.5 °C .
- 10- Frost surface temperature is measured by a digital infrared thermometer (SCANTEMP 410) with a resolution of 0.1 °C and accuracy of ±1 °C .
- 11- Frost thickness is measured by a digital micrometer with accuracy of ±0.004 mm.
- 12- After a fixed time (10 min) the next reading is recorded with the previous sequence every 10 min until reaching total experimental time (120 min).

3. Data Reduction

To perform the required analysis of the study, the experimental data before and after the tested cooled plate inside the test section were measured. The measurements include temperature and air relative humidity at inlet and outlet of the test section, and the mean velocity at each run, one can evaluate the value of local and average Nusselt and Sherwood numbers accomplishing the following procedures.

One can calculate the mass flow rate of the moist air (kg/s) by the following relation

$$\dot{m}_a = A \cdot u_{av} \cdot \rho_a \quad , (\text{kg/s}) \quad (1)$$

Where A is the cross sectional area of the air duct (m²), u_{av} is the average air velocity at

the test section (m/s), ρ_a is the air density at the air inlet temperature (kg/m³).

One can evaluate the average heat and mass fluxes through the following relations:

$$q'' = (\dot{m}_a / A_s) \cdot \Delta i(t) \quad , (\text{W/m}^2) \quad (2)$$

$$m'' = (\dot{m}_a / A_s) \cdot \Delta w(t) \quad , (\text{kg/m}^2\text{s}) \quad (3)$$

Where q'' is heat flux (W/m²), m'' is the mass flux (kg/m²s), A_s is the surface area of the cooled plat (m²), Δi and Δw are the difference of the total enthalpy and humidity ratio between inlet and outlet moist air and t is the loop time duration for each reading (s), respectively.

The enthalpy i (kJ/kg) and humidity w (kg_{wv}/kg_{da}) are determined from air psychometric tables [18], as the dry and wet bulb temperatures at the inlet and outlet of the considered section are known. The Local heat and mass coefficients can be calculated by the following formulas,

$$h(t) = q''(t) / (T_a - T_{fs}) \quad (\text{W/m}^2\text{k}) \quad (4)$$

$$h_m(t) = m''(t) / (\rho_a - \rho_{fs}) \quad , (\text{m/s}) \quad (5)$$

Where $h(t)$ is local heat transfer coefficient (W/m²k), $h_m(t)$ is local mass transfer coefficient (m/s), T_a is the average moist air temperature (k), T_{fs} is the frost surface temperature (k), ρ_{fs} is the density of saturated vapour at frost surface temperature (kg/m³), and ρ_a is the density of super-heated water vapor far from the cooled plat (kg/m³). Then, calculating local Nusselt and Sherwood numbers by:

$$Nu(t) = h(t) \cdot L / K \quad (6)$$

$$Sh(t) = h_m(t) \cdot L / D \quad (7)$$

Where L , K , D are the cooled plat length (m), thermal conductivity of the air (W/mk), and moist air mass diffusion coefficient at definite local time (m²/s), respectively.

Reynolds numbers by:

$$Re = (u_{av} \cdot L) / \nu_a \quad (8)$$

Where N and ν_a are the total number of time steps per each run and kinematic viscosity at mean air temperature (m^2/s), respectively.

4. Results and Discussion

The present experimental results sensitivity with respect to the operating conditions (dry-bulb temperature, air velocity and air relative humidity) are analyzed.

4.1 Validity of the experimental results

Validation of the experimental results is accomplished by comparison of average frost layer thickness, an important indicator

for monitoring the frost growth, with the previous experimental data. Figure (4) show the average frost thickness of the present experimental results and the data of Hermes et al. [19]. In general the frost thickness is increase with increasing time. The obtained experimental results and the previous works gave the same trend. In general the maximum deviation is 19.2% at the time end. The deviation between the present and previous work due to the plate dimension difference between them.

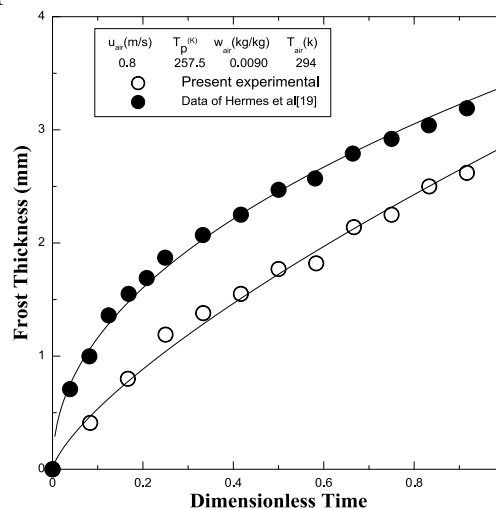


Fig.(4) Comparison between the present experimental data and data of Hermes et al.[19]

4.2 Effect of Plate Surface Temperature on Frost layer thickness

The effect of plate surface temperature is analyzed, keeping the air flow conditions constant. Figure (5) Shows the effect of the plate surface temperature on frost layer thickness, and heat and mass transfer coefficients.

Figure (5-a) shows the effect of the plate surface temperature on frost layer thickness. The frost layer thickness increases with decreasing the plate surface temperature. While this can be partially explained by the fact that decreasing the plate surface temperature increases the heat transfer coefficient, which also increases the mass transfer coefficient thus causing the frost deposition rate increase. Figure (5-b) shows the effect of the

plate surface temperature on heat transfer coefficient. The heat transfer coefficient decreases continuously during frost formation as the surface temperature of the frost layer increases with increasing of frost layer thickness. The heat transfer coefficient increases with decreasing the plate surface temperature, because increasing the temperature difference between air temperature and surface temperature of the frost layer. The same effect of the plate surface temperatures on the mass transfer coefficient is showing in Fig. (5-c).

4.3 Effect of Air Humidity on Frost Layer

Figure (6) shows the effect of the air humidity on frost layer thickness and heat and mass transfer coefficients.

Figure (6-a) shows the effect of the air humidity on frost layer thickness. One can found that the increasing of air humidity causes the driving potential of mass transfer between the air and frost surfaces to become large and, hence, the thickness of frost layer is increased.

The same effect of air humidity on heat and mass transfer coefficients are showing in Fig. (6-b) and Fig. (6-c) in respectively.

4.4 Effect of Dry Bulb Temperature of Air on Frost Layer

Figure (7) shows the effect of the air temperature on frost layer thickness, and heat and mass transfer coefficients.

Figure (7-a) shows the effect of the dry blub temperature of air on frost layer thickness. It is found that the no effect of the dry blub temperature of air on frost thickness, because the driving potential of mass transfer between the air and frost surfaces to become constant, hence, the thickness of frost layer is not changed. The same effect of the dry blub temperature of air on the mass transfer coefficient is showing in Fig. (7-c).

Figure (7-b) shows the effect of the dry blub temperature of air on heat transfer coefficient. One can found that the increasing of the dry blub temperature of air causes the temperature gradient between the air and frost surfaces to become large and,

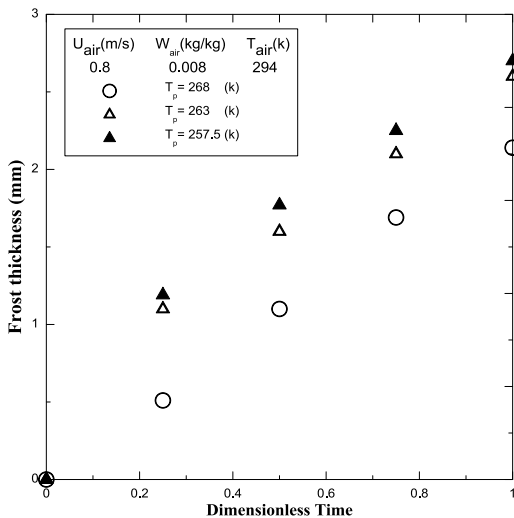


Fig. (5-a) Relation between frost thickness with dimensionless time.

hence, the heat transfer coefficient is increased.

4.5 Effect of Air Velocity on Frost Layer

Figure (8) shows the effect of the air velocity on frost layer thickness, and average heat and mass transfer coefficients.

Figure (8-a) shows the effect of the air velocity on frost layer thickness. The results show that the frost layer thickness increases with increasing air velocity. The frost layer grows rapidly due to the active mass transfer. It could be explained by the analogy between heat and mass transfer on the frost surface, since heat transfer actively takes place with an increasing Reynolds number by increasing air velocity.

5. Conclusions

The present experimental results compare well with the previous test data. It is revealed that the plate surface temperature has the greatest effect on frost thickness, heat and mass transfer coefficients. Plate surface temperature and air velocity they have considerably larger effect on frost thickness relative to the air humidity and dry bulb temperature of air. The experimental result shows that the dry bulb temperature of air does not have appreciable effect on frost thickness, and mass transfer coefficient. The air humidity slightly increases the frost layer thickness and mass transfer coefficient.

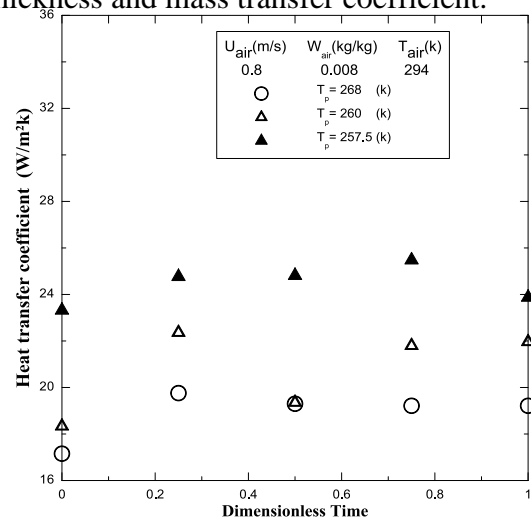


Fig. (5-b) Relation between heat transfer coefficient with dimensionless time.

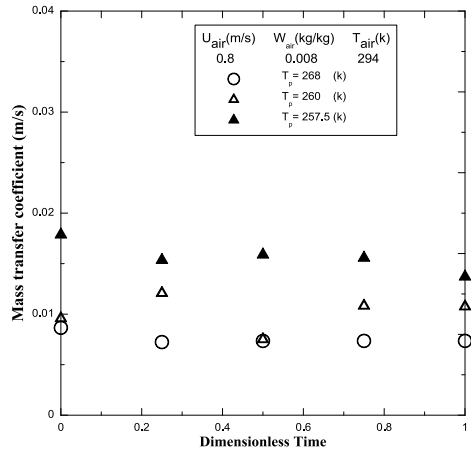


Fig. (5-c) Relation between mass transfer coefficient with dimensionless time.

Fig. (5) Effect of Cold plate temperature on the frost layer properties.

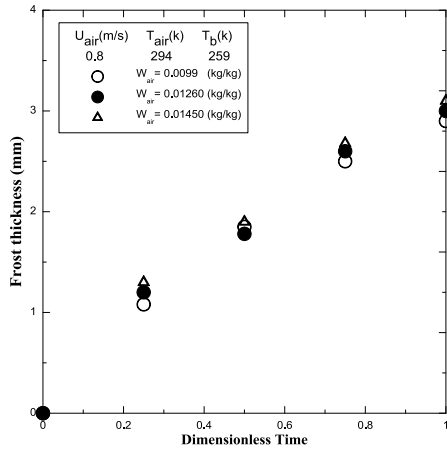


Fig. (6-a) Relation between frost thickness with dimensionless time.

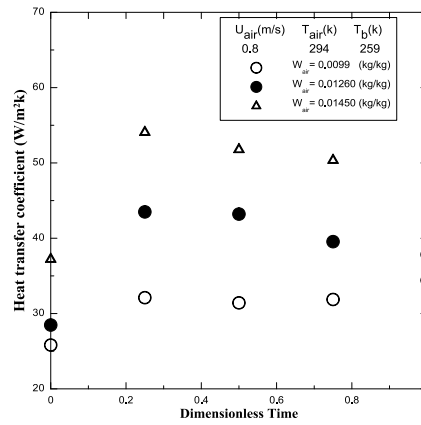


Fig. (6-b) Relation between heat transfer coefficient with dimensionless time.

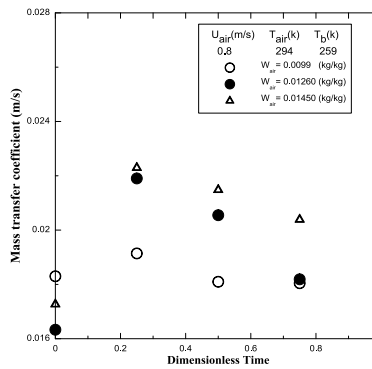


Fig. (6-c) Relation between mass transfer coefficient with dimensionless time.

Fig. (6) Effect of air humidity on the frost layer properties.

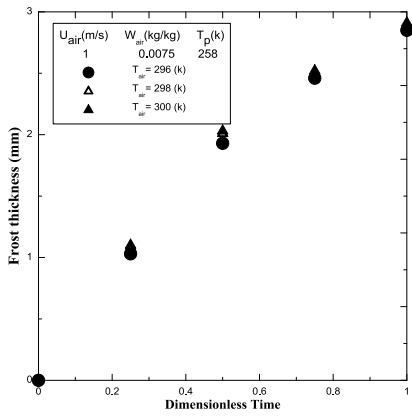


Fig. (7-a) Relation between frost thickness with dimensionless time.

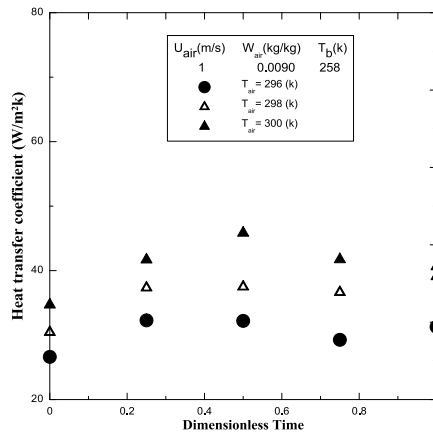


Fig. (7-b) Relation between heat transfer coefficient with dimensionless time.

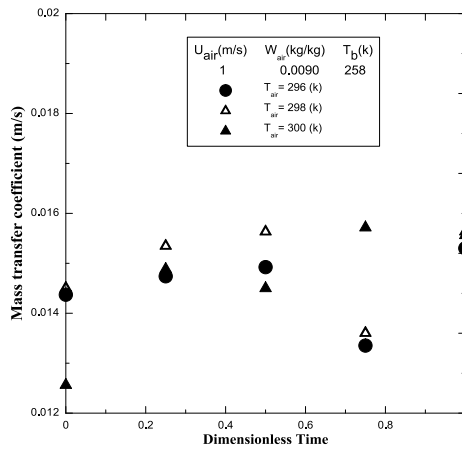


Fig. (7-c) Relation between mass transfer coefficient with dimensionless time.
 Fig.(7) Effect of dry bulb temperature of air on the frost layer properties.

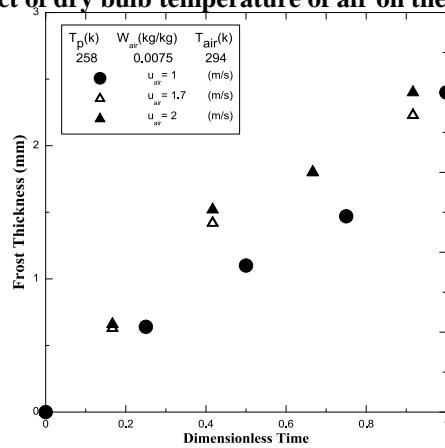


Fig. (8) Effect of air velocity on the frost layer properties.

Reference

- [1] Kennedy L.A. and Goodman J., "Free convection heat and mass transfer under conditions of frost deposition", *Int. J. of Heat and Mass Transfer* 17, No. (4), pp.477-484, (1974).
- [2] Hayashi Y., Aoki A., Adachi S. and Hori K., " Study of frost properties correlating with frost formation types", *J. Heat Transfer* 99 ,PP.239–245, (1977).
- [3] Schneider H. W., "Equation of the growth rate of frost forming on cooled surfaces", *Int. J. of Heat and Mass Transfer* 21, No. (8), pp. 1019-1024, (1978).
- [4] Marinyuk B. T., "Heat and mass transfer under frosting conditions", *Int. J. of Refrigeration*, 3, No. (6), pp. 366-368, (1980).
- [5] Dietenberger M.A., "Generalized correlation of the water frost thermal conductivity", *Int. J. of Heat and Mass Transfer*, 26, No. (4), pp. 607-619, (1983).
- [6] Sami S. M. and Duong T., "Numerical prediction of frost formation on cooled heat exchangers" *Int. J. of Heat and Mass Transfer*, 15, No. (1), pp. 81-94, (1988).
- [7] Östin R. and Andersson S., "Frost growth parameters in a forced air stream" *Int. J. of Heat and Mass Transfer*, 34, No. (4-5), pp. 1009-1017, (1991).
- [8] Östin R., "A study of heat exchange under frosting conditions" *Heat Recovery Systems and CHP*, 12, No. (2), pp. 89-103, (1992).
- [9] Tao Y.X., Besant R.W. and Rezkallah K.S., "A mathematical model for predicting the densification and growth of frost on a flat plate" *Int. J. of Heat and Mass Transfer*, 36, No. (2), pp. 353-363, (1993).
- [10] Sherif S. A., Raju S. P., Padki M. M. and Chan A. B., "A semi-empirical transient method for modeling frost formation on a flat plate", *Int. J. of Refrigeration*, 16, No. (5), , pp. 321-329, (1993).
- [11] Le Gall R., Grillot J. M. and Jallut C., "Modeling of frost growth and densification", *Int. J. of Heat and Mass Transfer*, 40, No. (13), pp. 3177-3187, (1997).
- [12] Lee K.S., Kim, W.S., Lee, T.H., " A one-dimensional model for frost formation on a cold flat surface". *Int. J. Heat Mass Transfer* 40, 4359-4365,(1997).
- [13] Ismail K.A.R., Salinas C., Gonc M.M. and alves, "Frost growth around a cylinder in a wet air stream", *Int. J. Refrig.* 20,No. (2),PP. 106–119, (1997).
- [14] Wu X. M. and Webb R.L., "Investigation of the possibility of frost release from a cold surface", *Experimental Thermal and Fluid Science*, 24, No. (3-4), pp. 151-156, (2001).
- [15] Cheng C. and Cheng Y., " Predictions of frost growth on a cold plate in atmospheric air ", *Int. Communications in Heat and Mass Transfer*, 28, No. (7), pp. 953-962, (2001).
- [16] Fossa M., and Tanda G., "Study of free convection frost formation on a vertical plate", *J. of Experimental Thermal and Fluid Science* 26, pp. 661–668, (2002).
- [17] Wang W., Guo Q.C., Lu W.P., Feng Y.C. and Na W., "A generalized simple model for predicting frost growth on cold flat plate", *Int. J. of Refrigeration*,35, pp. 475-486, (2012).
- [18] Dennis L. O'Neal "ASHRAE Hand book Fundamentals ", *hand book*, ASHRAE Foundation,(2009).
- [19] Hermes, Christian J.L., Piucco, Robson O., Barbosa Jr., Jader R.,Melo and Cláudio., "A study of frost growth and densification on flat surfaces". *Exp. Therm. Fluid Sci.* 33, 371-379, (2009).

